

GRAVITATING LIGHT BALL: STATIONARY STATES AND COLLAPSE DEVELOPING

S.N. SOKOLOV

Institute of High Energy Physics, Protvino

Moscow Region, 142284, Russia

ABSTRACT. *Equations of motion convenient for numerical solution are deduced within the frame of GR in a spherically symmetric case for a ball filled with light-gas. It is also shown that the variables of the gravitational field can be eliminated from the equations of motion converting the gravitational interaction into the equivalent direct interaction of matter with itself. Stationary states, oscillation modes and instability modes are computed, and processes of decay of "hot" states and collapse are studied.*

INTRODUCTION

The pressure of light grows with temperature as T^4 - faster than the pressure of any massive matter - and is the most important factor of dynamics of the heaviest and hottest celestial objects. So it is reasonable to single out this factor and to analyze the behaviour of the pure light in the gravitational field that it creates. In this paper we consider the static distribution and the collapse of the thermal radiation in a large spherical black cavity. If the walls of the cavity are thin and weigh little, it can be viewed as a large balloon filled with light - a light ball.

The static equilibrium of a spherical light ball in the frame of GR was analyzed in (Sorkin et al., 1981), where the main attention was paid to the entropy of the equilibrium states. It was found that depending on the ratio M/R at the surface of the ball it might have no equilibrium states at all, or have one or more such states corresponding to the local extrema of the entropy. Referring to the theory of stability (Weinberg, 1972), Sorkin et al. (1981) demonstrated that among the equilibrium states of the light ball only the coolest one is stable.

In the present paper we reproduce in a more direct way some of the results of

Sorkin et al. (1981) and go further:

- look for the static solutions that have any mass and surface temperature;
- formulate the spherically symmetric nonstatic problem;
- find spherical instability modes near the equilibrium states;
- compute the propagation of a local perturbation of unstable static state;
- demonstrate how an unstable state decays (collapses or anticollapses).

In the static case, the pressure P and the energy density W of the black-body radiation obey the law

$$P = aT^4, \quad W = 3P, \quad (1)$$

where

$$a = 8\pi^5 k^4 / 15c^3 h^3 = 7.5 \cdot 10^{-15} \text{ erg/cm}^3 \cdot \text{grad}^4,$$

and T is measured in Kelvin. In the nonstatic case the notion of temperature and the state equation (1) can be used, only if a local thermal equilibrium is reached fast enough compared to the changes of other values. We will suppose that a small amount of dust or other scattering agents are present inside the ball, so the radiation length is small enough, the black-body radiation behaves like a light-gas, and the state equation (1) is always true.

We will consider only spherical configurations of matter and use the standard coordinates

$$g_{\mu\nu} = \text{diag}\{-D(t,r), A(t,r), r^2, r^2 \sin^2\theta\}. \quad (2)$$

EQUATIONS OF MOTION

In GR the gravitational interaction of matter obeys the Einstein-Hilbert equations

$$\tilde{R}^{\mu}_{\nu} = -8\pi G T^{\mu}_{\nu}, \quad (3)$$

where $G = 6.67 \cdot 10^{-8} \text{ cm}^3 \text{ g}^{-1} \text{ s}^{-2}$, and T is the energy-stress tensor of matter. The Einstein tensor for metric (2) is

$$\tilde{R}^{\mu}_{\nu} = \begin{pmatrix} \frac{1-(r/A)'}{r^2} & \frac{\dot{A}}{ADr} & 0 & 0 \\ -\frac{\dot{A}}{A^2 r} & \frac{1-1/A-rD'/(AD)}{r^2} & 0 & 0 \\ 0 & 0 & E_2^2 & 0 \\ 0 & 0 & 0 & E_3^3 \end{pmatrix}, \quad (4)$$

where $A' = \partial A / \partial r$, $\dot{A} = \partial A / \partial t$, etc., and

$$E_2^2 = E_3^3 = \frac{1}{4} \left(\frac{2\dot{A}}{AD} - \frac{\dot{A}^2}{A^2 D} - \frac{\dot{A}\dot{D}}{AD^2} + \frac{A'D'}{A^2 D} + \frac{2A'}{A^2 r} - \frac{2D''}{AD} + \frac{D'^2}{AD^2} - \frac{2D'}{ADr} \right).$$

The stress-energy tensor for the light-gas moving radially with velocity $v = \text{th}[u(t,r)/2]$ is

$$T_{\nu}^{\mu} = p\delta_{\nu}^{\mu} + (W+p)U^{\mu}U_{\nu},$$

where $U_{\mu} = \{-\text{ch}(u/2)\sqrt{D}, \text{sh}(u/2)\sqrt{A}, 0, 0\}$, so

$$T_{\nu}^{\mu} = p \begin{pmatrix} -2\text{chu}-1 & +2\sqrt{A/D}\text{shu} & 0 & 0 \\ -2\sqrt{D/A}\text{shu} & 2\text{chu}-1 & 0 & 0 \\ 0 & 0 & 1 & 0 \\ 0 & 0 & 0 & 1 \end{pmatrix}. \quad (5)$$

Equation (4) gives 4 independent equations

$$\frac{1-(r/A)'}{r^2} = p(2\text{chu}+1), \quad (6.1)$$

$$\frac{\dot{A}}{ADr} = -2p\sqrt{A/D}\text{shu}, \quad (6.2)$$

$$\frac{1-1/A-rD'/(AD)}{r^2} = -p(2\text{chu}-1), \quad (6.3)$$

$$E_2^2 = -p, \quad (6.4)$$

where $p = 8\pi G\rho$, for 4 unknown functions $A(t,r)$, $D(t,r)$, $p(t,r)$, $u(t,r)$. This system is rather messy, especially the latter equation, containing A, D'' . An equivalent, but more clear system can be obtained, if equations (6.2), (6.4) are replaced by the linear combinations of all equations (6) - by the covariant divergences of both sides of (4):

$$\tilde{R}_{t;\mu}^{\mu} = -8\pi G T_{t;\mu}^{\mu}, \quad \tilde{R}_{r;\mu}^{\mu} = -8\pi G T_{r;\mu}^{\mu}.$$

Due to the Bianci identities, the left-hand sides of these equations vanish, and we have two equations

$$T_{t;\mu}^{\mu} = 0, \quad T_{r;\mu}^{\mu} = 0, \quad (7)$$

containing \dot{p} , \dot{u} . Solving system (7) for \dot{p} , \dot{u} and using equation

$$\dot{A} = -2\sqrt{A/DADr}\rho\text{shu}, \quad (6.2a)$$

(stemming from (6.2)) to exclude \dot{A} , we obtain

$$\dot{p} = \sqrt{\frac{D}{A}} \frac{1}{2+chu} \left\{ -p' shu + p \left[4shu \left(Apr \frac{1}{r} - \right) - 2u' \right] \right\}, \quad (8.1)$$

$$\dot{u} = -\sqrt{\frac{D}{A}} \left(\frac{D'}{D} + \frac{\frac{3p'}{2p} + 2\frac{1-chu}{r} + u' shu - 2Aprsh^2u}{2 + chu} \right). \quad (8.2)$$

These equations combined with equations (6) can be rewritten as

$$\frac{A'}{A} = -\frac{A-1}{r} + Apr(2chu+1), \quad (9.1)$$

$$\frac{D'}{D} = \frac{A-1}{r} + Apr(2chu-1), \quad (9.2)$$

make 4 first-order partial derivative equations suitable for analysis and numeric solution.

The systems (8), (9) are rather curious. The functions p, u describing the state of the matter play there a more fundamental role than the metric elements D, A . From the mathematical point of view, the knowledge of functions $p(t_0, r)$, $u(t_0, r)$ is sufficient for the computation of $D(t_0, r)$, $A(t_0, r)$, $\dot{p}(t_0, r)$, $\dot{u}(t_0, r)$, and completely defines the evolution of matter.

Indeed, using $p(t_0, r)$, $u(t_0, r)$ (and the regularity condition $A(t, 0)=1$) we can solve (9.1) and find $A(t_0, r)$, then solve (9.2) and find $D(t_0, r)$ (the unessential normalization factor can be set by the relation

$$D(t_0, r_3) = 1/A(t_0, r_3)$$

on the surface of the ball). After that \dot{p} , \dot{u} at $t=t_0$ are immediately computable.

From the physical point of view, the entities D, A , since they do not enter initial conditions, are *auxiliary* functions and can be excluded from the equations of matter evolution.

Indeed, defining a running mass $M(t, r)$ by the relation

$$A = 1/(1-M/r), \quad (10)$$

we can cast (9.1) to the form

$$M' = pr^2(2chu+1), \quad (11)$$

whence

$$M = \int_0^r p(2chu+1)r^2 dr. \quad (12)$$

Equation (9.2) gives

$$D = \text{const} \cdot \exp \left\{ \int_0^r \left[\frac{A-1}{r} + Apr(2chu-1) \right] dr \right\}. \quad (13)$$

Substitution of (10), (12), (13) into (8) transforms it into a set of tegrom differential equations for functions p , u only, describing the evolution of matter interacting *directly* with itself.

Equations (9) are curious in one more aspect. According to (9), an abrupt local perturbation of $p(t,r)$ near some point r_0 leads, formally, to the instant change of D everywhere and of A at $r \geq r_0$, which seems to violate the causality principle. Actually, the causality principle is not violated for two reasons. One of them is that equation (6.2) (which is always valid) clearly tells that a reacts to changes of p, u only locally. Another reason is that according to (9.2) after the perturbation only the normalizations of D within each region $r < r_0$ and $r > r_0$ are changed, and this effect cannot be noticed instantly: to measure the change in the ratio of the normalizations in the two regions, one has to wait for the arrival of a light signal from the other region. So, no signal moving faster than light can be transferred due to equations (9).

STATIONARY STATES

In the static case $\dot{p}=\dot{u}=u=0$, equation (8.1) becomes trivial and other equations reduce to

$$\frac{D'}{D} = - \frac{p'}{2p}, \quad (14)$$

$$\frac{A'}{A} = - \frac{A-1}{r} + 3Apr, \quad (15)$$

$$\frac{D'}{D} = \frac{A-1}{r} + Apr. \quad (16)$$

Equation (14) says that $p \sim 1/D^2$ and, together with (1), that $T^2 \sim 1/D$. It is just a particular case of the well-known fact that the equilibrium temperature in the gravitational field is not constant. Instead, the *visible* temperature at point y observed from point x does not depend on y

$$T(y;x) = T(y) \sqrt{g_{00}(y)/g_{00}(x)} = T(x).$$

If the observation point x is inside the light ball and the observed point y is a

its surface, the factor

$$\sqrt{g_{00}(y)/g_{00}(x)} > 1$$

and is a *blue* shift, due to which the temperature near the center of the light ball should be higher than at the surface. Substituting $p(r)=p_0 D(0)^2/D(r)^2$, where $p_c=p(0)$ is the pressure at the center, and using instead of D, A the functions

$$B(r)=M(r)/r = 1-1/A, \quad f(r) = D(0)^2/D(r)^2,$$

we rewrite (15), (16) as

$$\begin{aligned} B' &= 3p_c r f - B/r, \\ f'/2f &= -(B/r + p_c r f)/(1-B). \end{aligned} \tag{17}$$

Since $f(0)=1$ and $B(0)=0$, the boundary conditions in (17) at $r=0$ are completely fixed.

The system (17) has an exceptional solution

$$B_e = 3/7, \quad f_e = 7p_c/r^2 \tag{18}$$

that does not satisfy the condition $f(0)=1$. As we shall soon see, every solution $B(r)$ of (17) tends to B_e at $r \rightarrow \infty$, so B_e is an attractor.

Since photons are massless and the boundary conditions at the center do not contain any scale, equations (17) should be scale-invariant. Indeed, if $\{B(r), f(r)\}$ is the solution of (17), the couple of functions

$$\tilde{B}(r) = B(r\lambda), \quad \tilde{f}(r) = f(r, \lambda)$$

is the solution of (7) for the same initial conditions at $r=0$ and for p_c replaced by $\tilde{p}_c = p_c \lambda$. Therefore, it is sufficient to know the function $B_*(r)$ satisfying the parameter-free equations

$$B_*' = 3rf_1 - B_*/r, \quad f'/2f = -(B_*/r + rf)/(1-B_*) \tag{19}$$

with the conditions $B_*(0) = 0, f(0) = 1$: solution $B(r)$ of (17) for any p_c can be obtained from $B_*(r)$ with a scale transformation.

The functions B_*, f are easily computed numerically. The behaviour of f is better seen, if one plots $F=3r^2f$ instead of f (see Fig.1)

The function $B_*(r)$ starts to increase parabolically from zero, reaches at $r=1.92$ the maximum $B_{\max} = 0.493$, then slowly decreases and reaches at $r=11.6$ the first minimum $B_{\min} = 0.411$, and then slowly oscillating tends to the asymptotic value $B_{a3} = 3/7$. At large r

$$B_* \approx ar^{-3/4} \cos(\omega \ln(r/r_a)) + 3/7, \tag{20}$$

where $a \approx 0.119$, $\omega \approx (47/16)^{1/2}$, and $r_a \approx 1482$. The function F due to relation $F = B_* + r$ has a similar asymptotic.

The solution $B(r)$, $f(r)$ for the given $p_c = T(0)^4 a 8\pi G$ is

$$B(r) = B_1(r\lambda), \quad f(r) = f_1(r\lambda), \quad \lambda = \sqrt{p_c}. \quad (21)$$

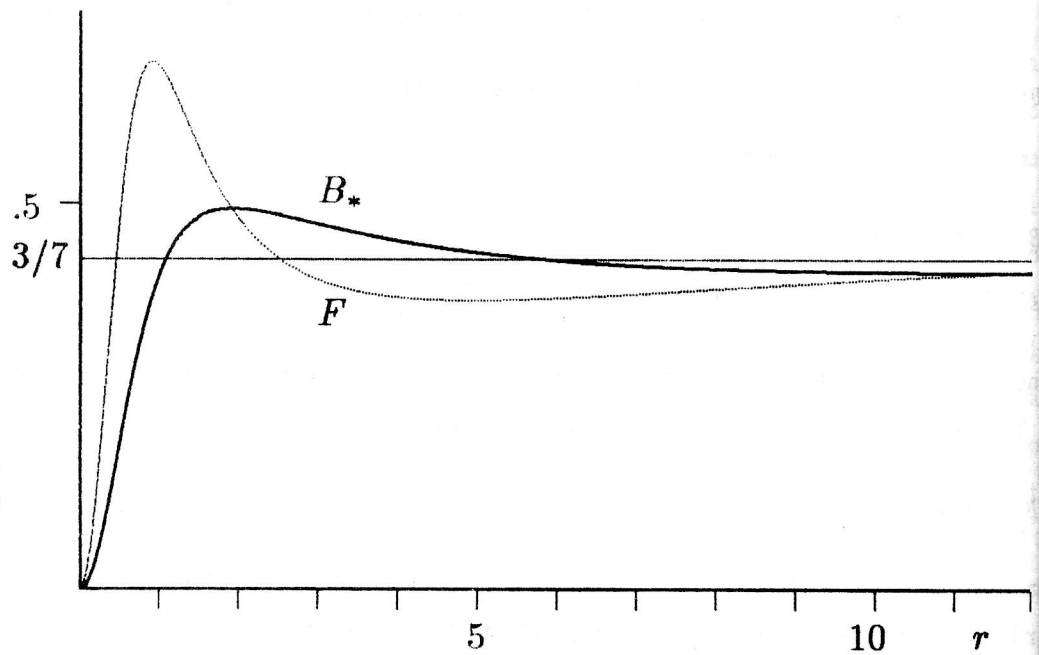


Fig.1. Basic solution of static equation.

At large r_0 and r every solution tends to the exceptional one, so it is an attractor. The exceptional solution B_e can be also considered as an improper limit of B at $p_c \rightarrow \infty$.

Let us return to the physically more interesting functions $D(r)$, $p(r) = p_c f(r)$. To find D , one has to fix the radius r_3 of the ball. Since outside the ball there is no matter and the Schwarzschild solution is true, we should have at the surface $D(r_3) = 1 - B(r_3)$. Hence,

$$D(r) = [1 - B(r_3)] \sqrt{f(r_3)/f(r)}.$$

The curves B, D and $T = 0.5 \cdot p^{1/4}$ for two states with the same mass and radius ($M = 0.4$, $r_3 = 1$) are given in Fig.2. The temperature at the center for the hot solution is three times larger than for the cool one.

STATIONARY SOLUTIONS CONTINUED FROM THE SURFACE

In case of cosmic objects observed from outside, it is more natural to use as a known parameter not the temperature at the center, but rather the total mass $M_\infty = M(r_3)$ and the temperature $T_3 = T(r_3)$ at the surface of the body. Due to the regularity condition $B(0) = 0$, the only free parameter is $T(0) \sim p_c^{1/4}$ and the values

$$B_3(p_c) = B_1(r_3 \sqrt{p_c}),$$

$$T_3(p_c) = p_c^{1/4} f_1(r_3 \sqrt{p_c})$$

make a 1-parameter family (see the spiral-like curve in Sorokin et al., 1981). The natural question arises which solution of equations (15), (16) correspond to M_∞ and T_3 not belonging to this family.

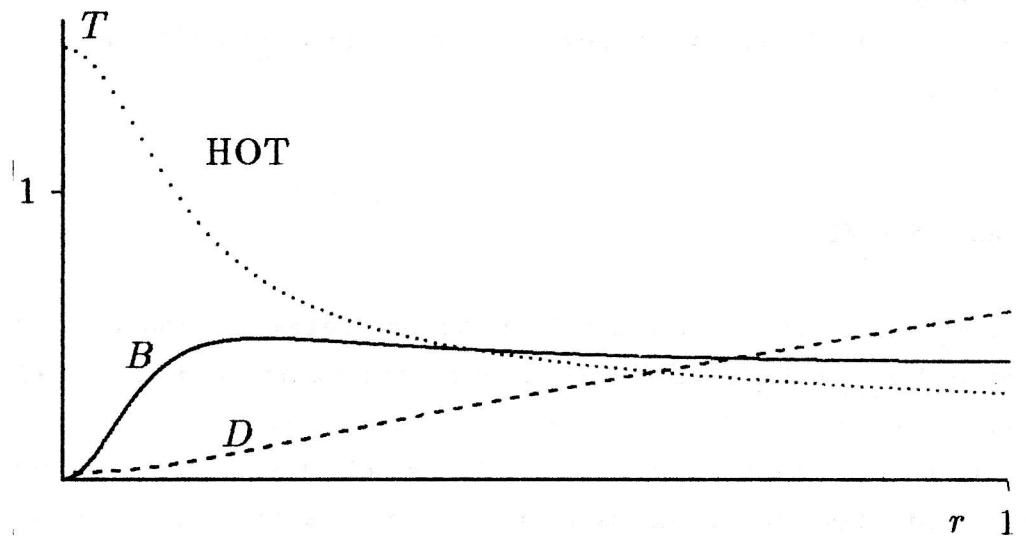
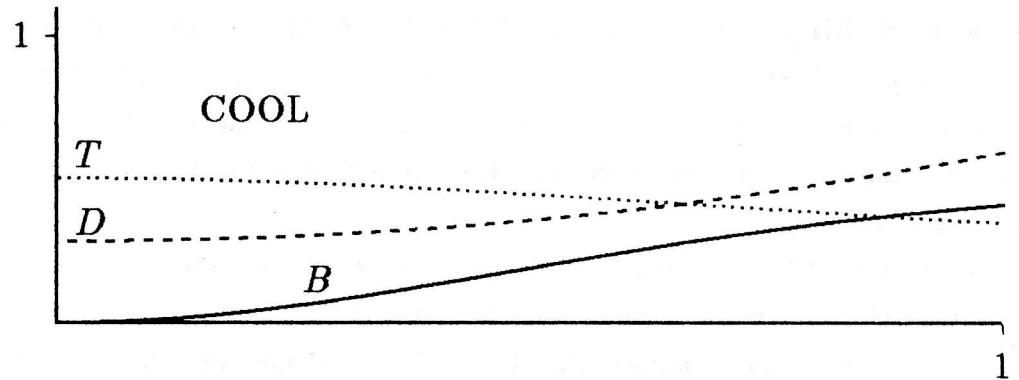


Fig.2. Two states with the same mass and radius.

Three typical solutions of (15), (16) are drawn in Fig.3.

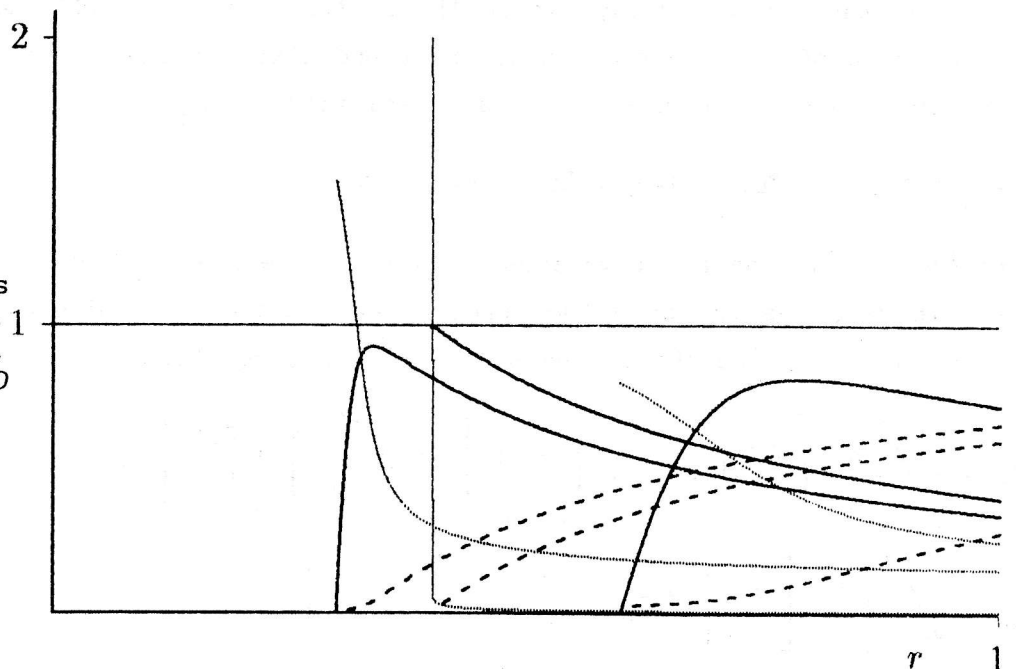


Fig.3. Three states in spherical layers. Thick curves - B , thin - T , dashed - D . $B=0$ at $r=0.3, 0.6$. $T=\infty, B=1$ at $r=0.4$.

The solutions continued from the surface toward the center generally do not reach it at some point r_* , either the mass $M(r)$ (and function $B(r)$) becomes zero, or function $B(r)$ reaches 1 and the temperature $T(r) = T_3 \sqrt{D(r_3)/D(r)}$ becomes infinite. Such solutions describe the static distribution of the black-body radiation not in the globe but in the spherical layers enclosed between two hard spheres of radii $r_1 > r_*$ and r_3 . The value $M_1 = B(r_1)r_1$ is the mass of the inner sphere and $T(r_1)$ is the temperature of its surface. If $B(r_1)$ is close to 1, the radiation is condensed in a thin layer of the inner sphere, like an ocean on the surface of the Earth. To prevent the radiation from falling toward the center, the inner sphere should be hard enough to resist its pressure.

Now we are able to answer the question what happens in the original model (where the internal sphere is absent) if one pumps into the cavity too much radiation, so the ratio $B=M/r$ will exceed the limit B_{\max} . Since we know all the static solutions and among them there is none (neither regular, nor singular) with such B , the 'overdosed' radiation will never reach thermal equilibrium; the state will never become static.

UNSTABLE STATES

If M_∞ and r_3 of the light ball (here and below - without the internal sphere) are fixed and $B_{\min} < b < B_{\max}$, there are several solutions of $B(r)$ describing different physical states of the light ball with the same mass M_∞ (see Fig.2). As was pointed out (Sorkin et al., 1981), among these states only the coolest one (which is described by a monotonically increasing part of $B(r)$) is stable. The unstable states decay: the long-wave component of a small perturbation grows exponentially with time as $e^{t/\bar{t}}$. In the early stage of the decay, while the perturbation is still small, the decay time and the shape of decay harmonics can be found like the small oscillations.

Let the state be close to the static solution p_0, D_0, A_0 :

$$p = p_0 + \delta p, \quad u = \delta u, \quad D = D_0 + \delta D, \quad A = A_0 + \delta A,$$

where $\delta p, \dots$ and their derivatives $\delta \dot{p}, \delta p', \dots$ are small. Substituting this in (8.1), (8.2), (6.2a), keeping only the terms linear in $\delta p, \dots$, and excluding D'/D in (8.2) by means of (9.2), we obtain the system of three equations

$$\delta \dot{u} = -\sqrt{\frac{D_0}{A_0}} \left[\delta A \left(p_0 r + \frac{1}{r} \right) + \delta p \left(A_0 r - \frac{p'_0}{2p_0^2} \right) + \frac{\delta p'}{2p_0} \right],$$

$$\delta \dot{p} = \sqrt{\frac{D_0}{A_0}} \frac{p_0}{3} \left[\delta u \left(4A_0 p_0 r - \frac{4}{r} - \frac{p'_0}{p_0} \right) - 2\delta u' \right],$$

$$\delta \dot{A} = -2\delta u D_0 A_0 p_0 r \sqrt{A_0/D_0}.$$

Seeking oscillation solutions

$$\delta u = \bar{u}(r)\cos\omega t, \quad \delta p = \bar{p}(r)\frac{\sin\omega t}{\omega}, \quad \delta A = \bar{A}(r)\frac{\sin\omega t}{\omega},$$

expressing p'_0 through A_0 , p_0 with the help of (14), (16), and excluding \bar{A} from the equations for \dot{u}, \dot{p} , we finally obtain

$$\bar{u}' = \bar{u} \left(\frac{A_0^{-3}}{r} + 3A_0 p_0 r \right) - \bar{p} \frac{3}{2p_0} \sqrt{\frac{A_0}{D_0}}, \quad (22)$$

$$\bar{p}' = 2\bar{u}p_0 \sqrt{\frac{A_0}{D_0}} \left[\omega^2 + 2p_0 A_0 D_0 (p_0 r^2 + 1) \right] - 2\bar{p} \left(\frac{A_0^{-1}}{r} + 2A_0 p_0 r \right).$$

The regularity conditions in the center are:

$$\bar{u}(0) = \bar{p}'(0) = 0.$$

The boundary (normalization) condition is $\bar{p}'(0) = \text{const}$. In case of instability modes ω becomes imaginary, but equations (22) do not change: only parameter ω^2 becomes negative.

Fig. 4 shows the curves $\bar{p}(r)$, $\bar{u}(r)$ for several values of ω^2 . Clearly, if $\omega=0$, the knot of the function $\bar{u}(r)$ coincides with the point of maximal $B(r)$.

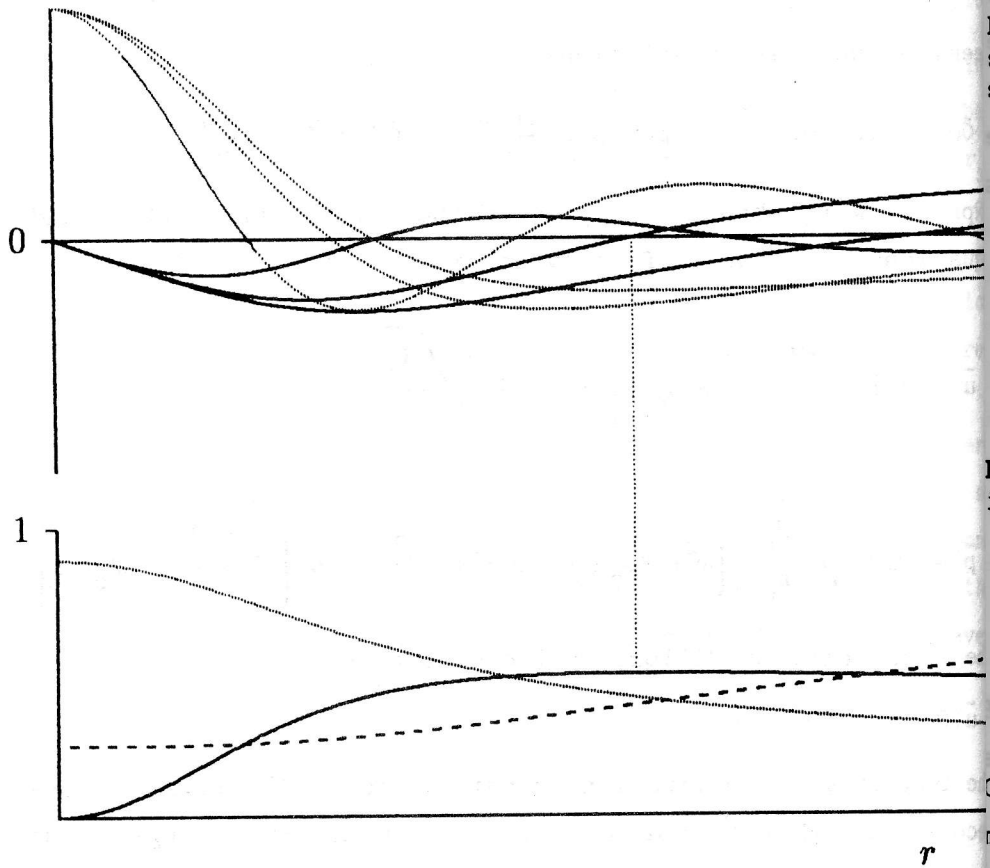
The proper values ω_n^2 are fixed by the condition $u(r_3)$. The oscillation mode with negative ω^2 exists only if the globe radius r_3 is greater or equal to the point r_u , where \bar{u} changes sign. One can also see that up to r_3 rather large compared to r_u only one instability mode (mode with $\omega^2 < 0$) exists.

DECAY AND COLLAPSE OF UNSTABLE STATE

Due to the nonlinearity of the equations of motion, any perturbation of an unstable state excites the instability mode and this mode starts to grow exponentially as $\text{sh}|\omega t|$. Depending on the sign of excitation, the state may evolve toward the cooler state, or evolve toward the hotter state and pass into collapse. The process is rich in details that are not easy to predict from general consideration. To have a closer look at the evolution of the light ball, the system of equations (8.1), (8.2), (6.2a), (9.2) was solved numerically with a number of initial states. One of the obtained movies is represented by a series of Figs. 5.0-5.9, where $v = \text{thu}/2$ (solid line), $T = 0.5 \cdot p^{1/4}$ (thin line), $B = M/r$ (dotted line), \sqrt{D} (dashed line), and $r_3 = 1$. The

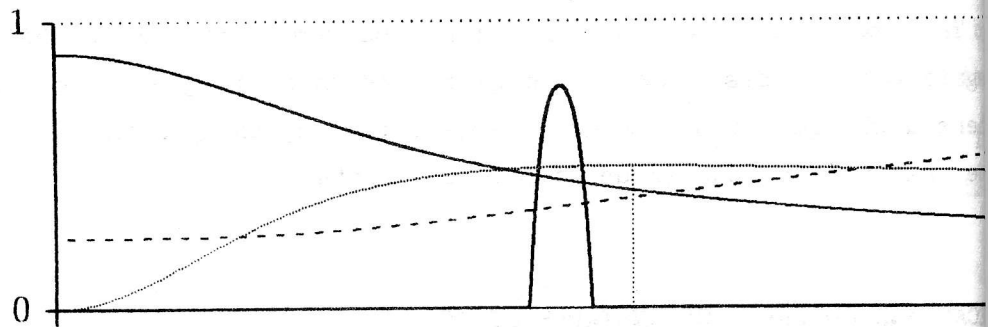
dotted vertical line indicated the maximum of B .

Fig.4. Oscillation and instability modes, $p(0)=10$. Upper part: $2\bar{u}$ (thick), \bar{p}/p (thin) for $\omega^2=4, 0, -0.7$. Lower part: B (thick), $\sqrt{D/A}$ (dashed), $T/2$ (thin).



The initial state (Fig.5.0, $t=0$) is an unstable stationary state locally perturbed by pushing a layer of light-gas toward the surface ($v>0$).

Fig.5.0. The initial state.



Soon (Fig.5.1, $t=0.2$) this push turns into two localized waves: compression wave moving toward the surface and decompression wave moving toward the center.

Since the push was strong - the initial velocity was greater than the velocity of sound $= 1/\sqrt{3}$ - both waves have steep shock fronts and are followed with tails of small oscillations. At $t=1$ the right wave is already reflected from the surface while the other wave is still approaching the center since, due to the factor $\sqrt{D/A}$ in (8), the speeds of light and of sound are smaller in the central region than near the surface.

At $t=2.6$ (Fig.5.2), the growth of the instability mode becomes well pronounced.

Fig.5.1. The compression and decompression waves.

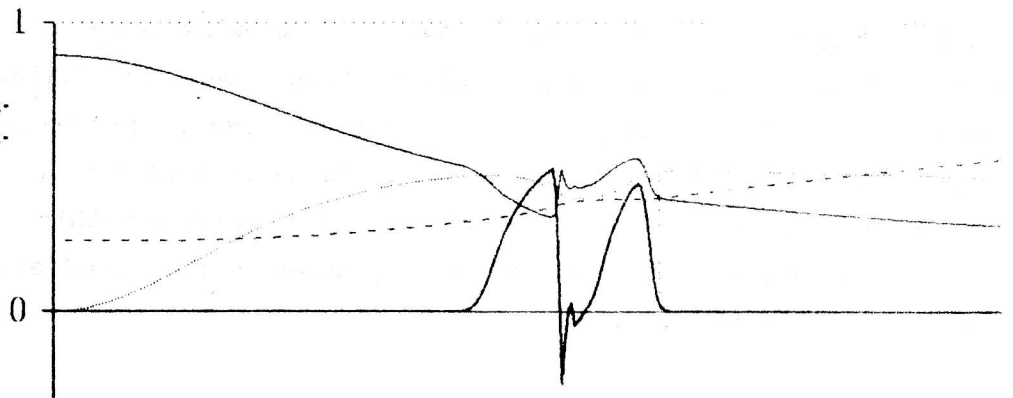
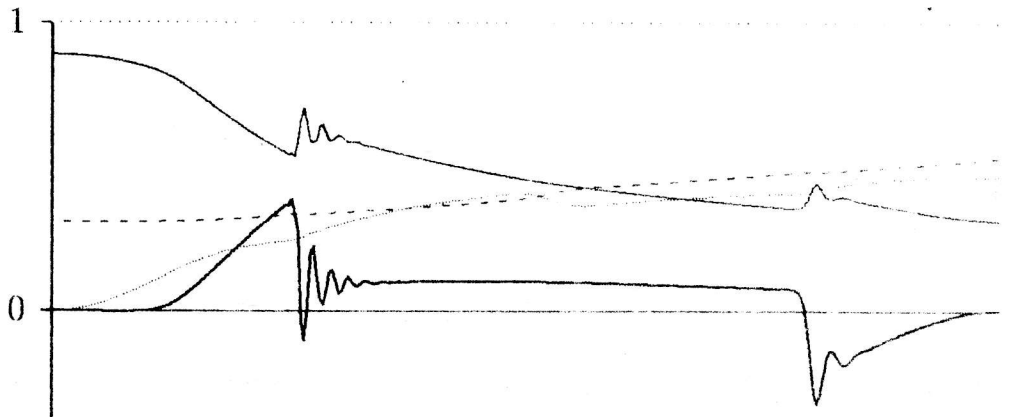


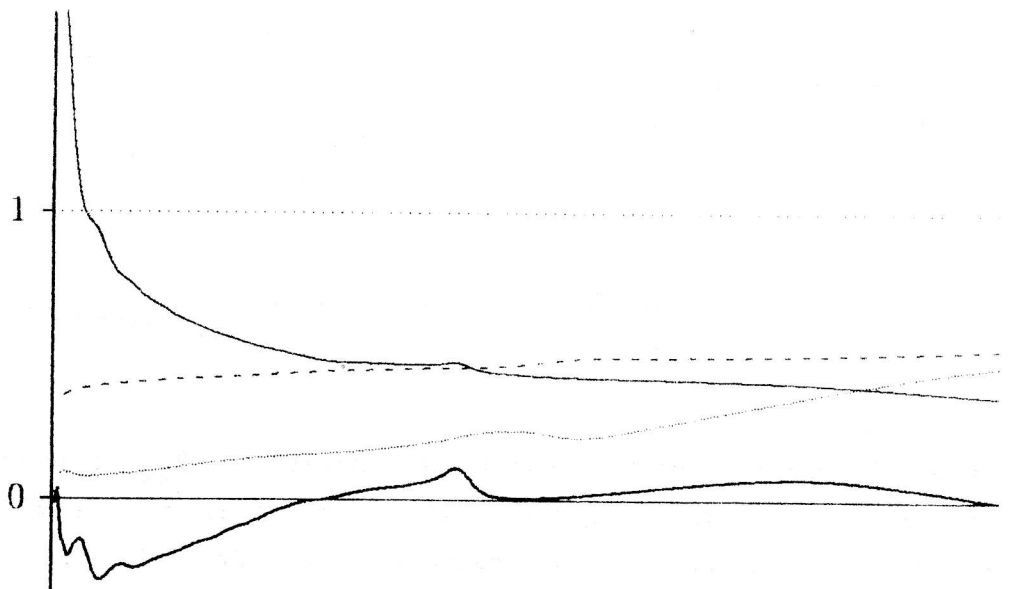
Fig.5.2. Growth of instability mode.



Of course, the initial perturbation, due to nonlinearity of the equations, excites many other oscillation modes, but they stay small and invisible, and only the instability mode shows up.

Next slide (Fig.5.3) at $t=3.9$ shows a high peak of pressure, when the left wave is reflected from the center and turns into a number of waves.

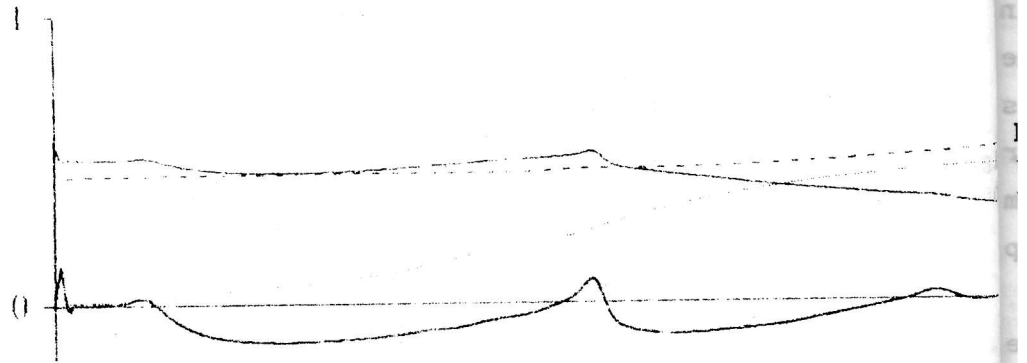
Fig.5.3. Reflection from the center.



This is one of the hard moments for the calculation procedure since, besides the growth of wave amplitude, the finiteness of step Δr (this movie was produced with $\Delta r=r_3/300$) excites the noise ultrasound waves concentrating near the center. To get a clean picture, one has to damp these ultrasound waves, which is done with the help of some smoothing local averaging of p and u equivalent to the admission of nonzero diffusion length and viscosity of the light-gas.

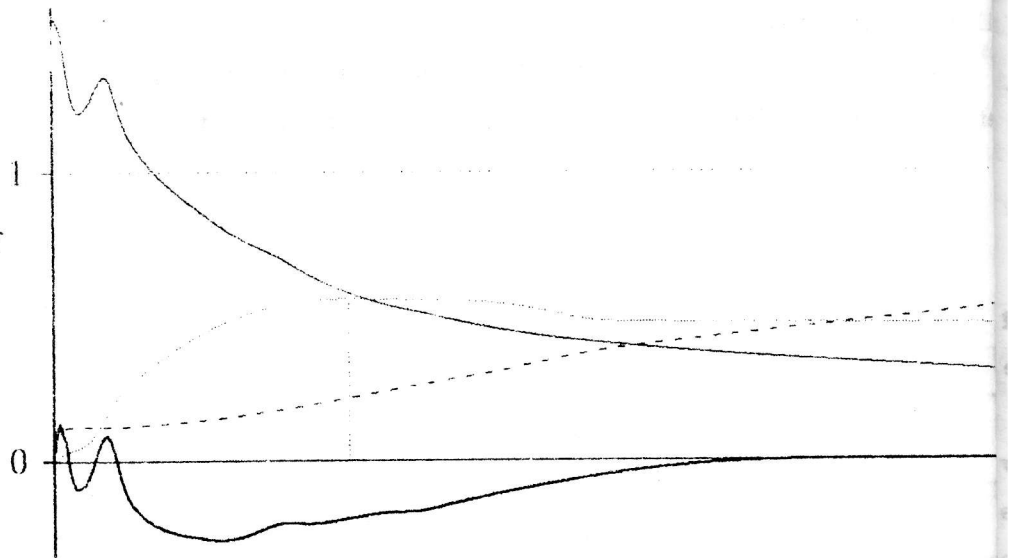
At $t=5$ (Fig.5.4), the instability wave stops growing and starts reflecting from the 8 surface. The state of the light ball at this moment is similar to the stable state in Fig.2. The stopping of the instability wave is an unrealistic feature of the model: in case of a star such a wave would cause an explosion and a shake-off of part of the mass. But here, since the light-gas is contained within a hard sphere and the shake-off is impossible, the instability wave is reflected and soon the light-gas starts moving toward the center.

Fig.5.4. The phase of quasi-homogeneous distribution.



At $t=9.8$ (Fig.5.5), the early stage of collapse is seen. The hump on the curve is forming. The speed of falling light-gas is about the speed of sound, so the waves from the center hardly move and gradually fade.

Fig.5.5. Beginning of collapse.



At $t=10.9$ (Fig.5.6), the collapse is well-developed, B_{\max} is about 0.77.

The speed of falling light-gas now reaches half of the velocity of light. The motion of waves in the internal region (to the left of the 'bottle-neck', where B is maximal) is practically stopped ($\sqrt{D/A} \sim 0$). This picture later does not change except that the light-gas in the external region is constantly sucked inside, B_{\max} approaches 1, and the temperature outside becomes lower and lower (Fig.5.7, $t=17$).

The speed of falling light-gas now reaches half of the velocity of light. The motion of waves in the internal region (to the left of the 'bottle-neck', where B

maximal) is practically stopped ($\sqrt{D/A} \sim 0$). This picture later does not change, except that the light-gas in the external region is constantly sucked inside, B_{\max} approaches 1, and the temperature outside becomes lower and lower (Fig.5.7, $t=17$).

Fig.5.6. Mid-collapse: time stops in the central region.

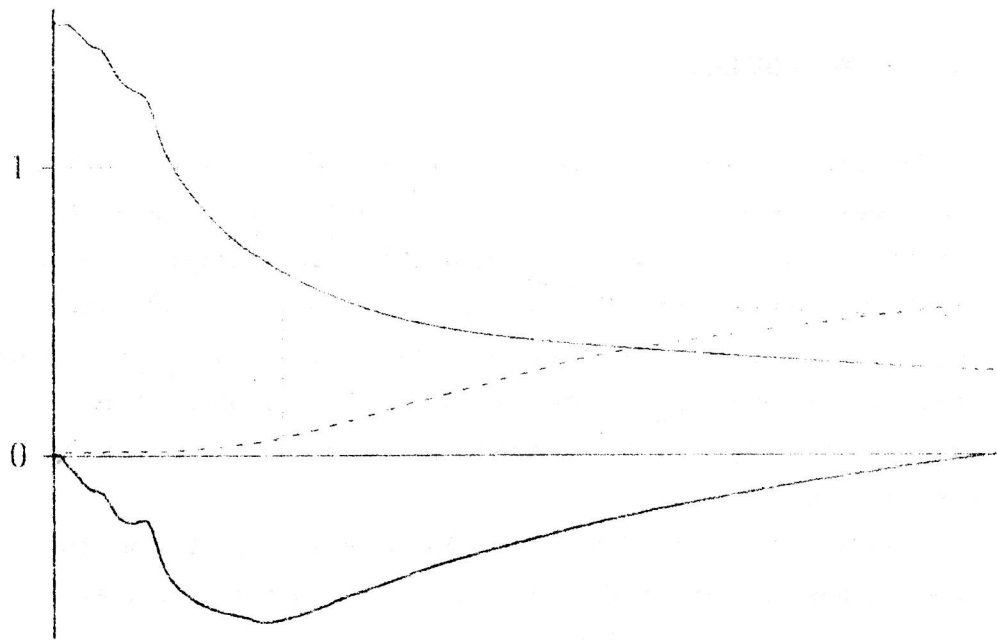
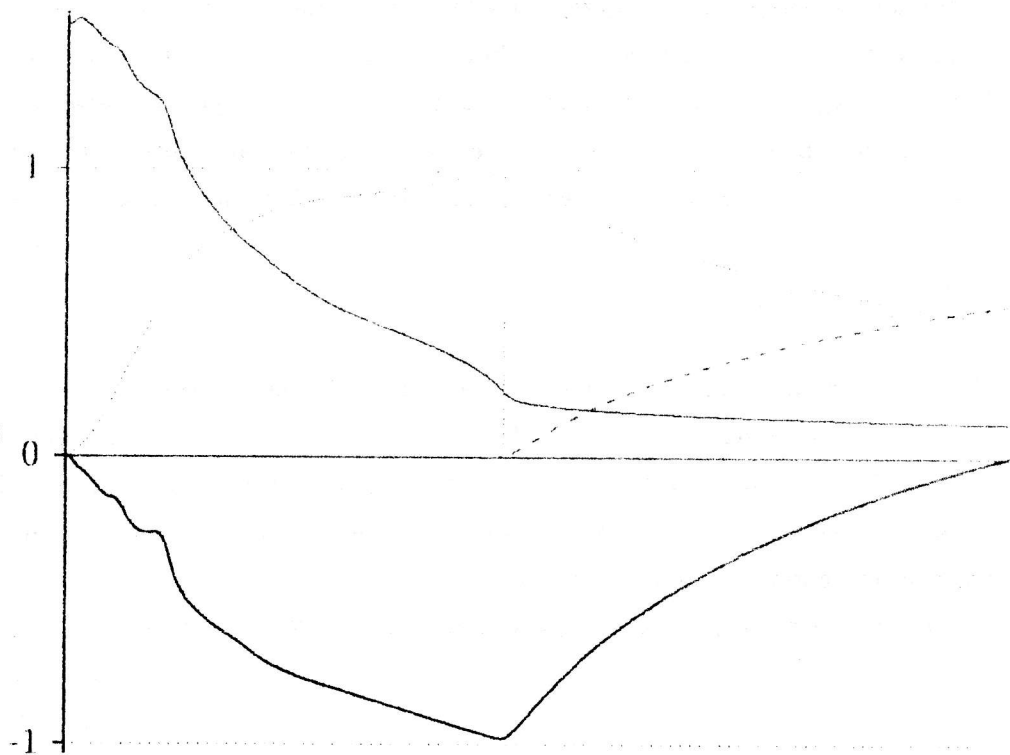


Fig.5.7. Late collapse: almost no light-gas in the outer region.



The model of ball with hard walls is rather unrealistic, so it is interesting to know what will happen in case of open light ball, having no walls. The calculation of evolution in an unlimited region of space needs a more complicated program, so as to obtain a preliminary picture of collapse of wallless ball, we imitated the absence of walls by changing the boundary conditions at the surface: we set $u'=0$ instead of $u=0$, thus letting the light-gas leave the sphere $r \leq 1$. We took the state of

mid-collapse as an initial state and repeated calculations. Without walls, the evolution was similar to that of a walled ball, only part of the light-gas near the boundary, was going off.

CONCLUDING REMARKS

The static and dynamical properties of the light ball are mainly in harmony with what was expected from crude estimates and general considerations. The main difference of the light-gas from the heavy matter is that the stable state of the light ball (the coolest solution) may have arbitrary large mass if the radius r_3 is large enough (only the ratio M/r is limited by $B_{\max}/2$). However, if the ratio $2M/r$ somewhere exceeds B_{\max} , the light ball collapses, turning into an object seen from outside as a dark ball of standard radius $r \sim 2M$. In the frame of GR, nothing can stop the collapse.

A self-gravitating light ball is a good object for the purpose of comparing the predictions of GR with predictions of other gravitational theories since it is sensitive to the relativistic and nonlinear terms in equations of motion and is reasonably easy to analyze numerically even in the nonstatic case. If a new theory claims to stop collapse of a heavy star, it should first be able to demonstrate it for the light ball. Same can be said for the supposed rebound.

A light ball may be considered as a crude approximation of a quark star. Indeed the matter in the quark star models is usually supposed to obey the law

$$P = \frac{1}{3}(W - 4b),$$

where b is a bounding energy density of the quark plasma. Except for the surface layer, where $W \sim 4b$, the properties of quark matter inside the star are close to those of the light-gas, so the quark star may be viewed as a light ball in an elastic bag. It would be interesting to calculate the oscillation modes of quark stars and compare them with those of the light ball.

The author is grateful to V.O.Soloviev, V.V.Sokolov, and V.Unt for discussions.

REFERENCES

- Sorkin R.D., Wald R.M., Zhang Z.J.: 1981, *Gen.Rel.Grav.*, **13**, No. 12, 1127-1146.
Weinberg S.: 1972, *Gravitation and Cosmology*. Wiley.